

## Magnetoresistance and magnetothermopower in the rhodium misfit oxide [Bi<sub>1.95</sub>Ba<sub>1.95</sub>Rh<sub>0.1</sub>O<sub>4</sub>][RhO<sub>2</sub>]<sub>1.8</sub>

Y. Klein, S. Hébert, D. Pelloquin, V. Hardy, and A. Maignan

*Laboratoire CRISMAT, UMR 6508 CNRS ENSICAEN, 6 bd Maréchal Juin, 14050 CAEN Cedex 4, France*

(Received 28 September 2005; revised manuscript received 10 March 2006; published 21 April 2006)

The magnetotransport properties of the Rh-based [Bi<sub>1.95</sub>Ba<sub>1.95</sub>Rh<sub>0.1</sub>O<sub>4</sub>][RhO<sub>2</sub>]<sub>1.8</sub> misfit oxide have been investigated. A metallic behavior is observed, coexisting with a large thermopower  $S$  of +95  $\mu\text{V}/\text{K}$  at room temperature, similar to what is observed in cobalt based misfit oxides. This  $S$  value can be explained by the coexistence of Rh<sup>3+</sup>(4 $d^6$ ) and Rh<sup>4+</sup>(4 $d^5$ ) in the RhO<sub>2</sub> layers, suggesting that they have the same influence as isoelectronic low spin state  $t_{2g}^6$ ,  $S=0$  Co<sup>3+</sup> (3 $d^6$ ) and  $t_{2g}^5$ ,  $S=1/2$  Co<sup>4+</sup> (3 $d^5$ ) in cobalt misfit oxides. From the specific heat measurements, the coefficient  $\gamma=38$  mJ K<sup>-2</sup> mol(Rh)<sup>-1</sup> shows that electron correlations are moderately strong. A small magnetoresistance is observed at low  $T$ , with two contributions, first negative up to 7 T, and positive for  $\mu_0 H > 7$  T, reaching +5% at 14 T and  $T=2.5$  K. This is a unique example of magnetoresistance in rhodium oxides, emphasizing the peculiarity of the transport properties arising from these CdI<sub>2</sub> type layers. The thermopower depends also strongly on field, with a magnetothermopower reaching -50% in 9 T at 2.5 K.

DOI: [10.1103/PhysRevB.73.165121](https://doi.org/10.1103/PhysRevB.73.165121)

PACS number(s): 71.27.+a, 72.15.Jf, 72.80.Ga, 75.47.Pq

### INTRODUCTION

Fascinating electronic properties can be found in transition metal oxides. In particular, the cobalt oxides family is very rich, due to the strong interplay between the structure and the valence and spin states of cobalt, responsible for the electronic properties of these phases. Among them, the Na<sub>x</sub>CoO<sub>2</sub> compound has been intensively studied due to its large thermopower coexisting with metallicity<sup>1</sup> and to its superconducting behaviour below  $T_c \sim 4.5$  K for the hydrated form.<sup>2</sup> These properties are strongly linked to the crystallographic structure, consisting of layers of edge-shared CoO<sub>6</sub> octahedra, in which the cobalt cations form a triangular array separated by deficient Na<sup>+</sup> layers. The coexistence of the large Seebeck coefficient ( $S$ ) together with metallicity has been investigated in a closely related family, the misfit cobalt oxides. They possess the same layers of tilted edge-shared octahedra, but separated, that time, by three or four rocksalt-like (RS) layers. By chemical substitution, optimization of the thermoelectric “figure of merit”  $Z=S^2/\rho\kappa$ , where  $\rho$  is the electrical resistivity and  $\kappa$  is the thermal conductivity, has been attempted (e.g., Refs. 3–5) and all oxide-thermoelectric generators with misfit cobalt oxides as  $p$ -type legs have already been designed for energy conversion of waste heat ( $T \gg 300$  K) into electricity.<sup>6</sup>

For all these compounds containing CoO<sub>2</sub> layers, the origin of the large thermopower coexisting with metallicity is still unclear. Two models had first been proposed. On the one hand, the Seebeck coefficient as  $T \rightarrow \infty$  has been calculated using a generalized Heikes formula;<sup>7</sup> due to the spin entropy, large  $S$  can be obtained for a mixture of Co<sup>3+</sup> and Co<sup>4+</sup> both in low spin states. On the other hand, a two-band model has been proposed<sup>8</sup> with two kinds of coexisting carriers, heavy ones with a peak in the density of states at the Fermi level responsible for the large Seebeck coefficient, and light ones responsible for metallicity. More recently, the importance of electron correlations for the large Seebeck has

been evidenced,<sup>9</sup> together with a spin entropy contribution to the thermopower.<sup>10,11</sup> The peculiar role of Co, of its electronic configuration and spin degeneracy, needs to be further investigated. In particular, substituting the Co directly in the conducting CoO<sub>2</sub> layer to understand its influence on transport properties is crucial. It has recently been shown that Rh, which can adopt a mixed valency Rh<sup>3+</sup>/Rh<sup>4+</sup> with 4 $d^6$ ( $t_{2g}^6$ ) and 4 $d^5$ ( $t_{2g}^5$ ) electronic configurations isoelectronic to Co<sup>3+</sup>/Co<sup>4+</sup>, can partially be substituted in Co in the CoO<sub>2</sub> layer in the Pb-based misfit oxides.<sup>12</sup> The thermopower remains large, but resistivity was changed to a more localized behavior. In a more recent study, the total substitution of Rh for Co has been evidenced in the BiBaRhO and BiSrRhO systems.<sup>13</sup> We focus here on the [Bi<sub>1.95</sub>Ba<sub>1.95</sub>Rh<sub>0.1</sub>O<sub>4</sub>][RhO<sub>2</sub>]<sub>1.8</sub> material in which a detailed investigation of its transport properties and their dependence on magnetic field has been made. These results are compared to those obtained for the corresponding cobalt misfit [Bi<sub>2</sub>Ba<sub>1.8</sub>Co<sub>0.2</sub>O<sub>4</sub>][CoO<sub>2</sub>]<sub>2</sub>.<sup>14</sup>

### EXPERIMENT

Samples of nominal composition Bi<sub>2</sub>Ba<sub>2</sub>Rh <sub>$b_1/b_2$</sub> O <sub>$a$</sub> , i.e., corresponding to the ideal  $n=4$  [Bi<sub>2</sub>Ba<sub>2</sub>O<sub>4</sub>]<sup>RS</sup>[RhO<sub>2</sub>] <sub>$b_1/b_2$</sub>  misfit phases ( $b_1/b_2$  is the misfit ratio of the  $b$  axis of the rocksalt and CdI<sub>2</sub> type, respectively), have been synthesized. According to these nominal chemical formulas, stoichiometric amounts of Bi<sub>2</sub>O<sub>3</sub>, BaCO<sub>3</sub>, and Rh<sub>2</sub>O<sub>3</sub> powders were mixed. First these mixtures have been heated at 800 °C during 12 h to eliminate carbonate groups. Then they were grounded again, pressed in the form of bars and set in alumina crucibles; then they were fired at 1000 °C for 24 h. Black ceramic bars were obtained.

The transmission electron microscopy has been performed by using a JEOL 2011CX FEG (200 kV) equipped with an EDAX analyzer.

Resistivity of the ceramic bars ( $1 \times 2 \times 6 \text{ mm}^3$ ) has been obtained using the four-probe measurement technique. Indium was ultrasonically deposited for electrical contacts. A physical properties measurement system (PPMS) from Quantum Design allows resistance measurements from 1.8 K to 400 K in the magnetic field ranging from 0 to 14 T. The thermoelectric power has been measured by a four point steady-state method with separated power and measuring contacts, using a homemade sample holder in the PPMS (1.8–320 K; 0–9 T). Specific heat measurements have been also carried out in the 9 T PPMS by using a  $2\text{-}\tau$  relaxation method. The magnetic properties have been studied with a dc SQUID magnetometer (1.8–400 K; 0–5 T) by recording magnetization as a function of temperature and magnetic field. The sample holder contribution has been measured separately and removed from the raw data.

## RESULTS

### Structural features

From electron diffraction (ED), a single phase is obtained for the nominal cationic composition “ $\text{Bi}_2\text{Ba}_2\text{Rh}_{1.9}$ .” In order to find evidence for the misfit features, electron diffraction patterns are shown in Figs. 1(a) and 1(b). The latter reveals a monoclinic composite lattice similar to the one observed in the case of the  $[\text{Bi}_2\text{Ba}_{1.8}\text{Co}_{0.2}\text{O}_4][\text{CoO}_2]_2$  modulated misfit cobaltite.<sup>14</sup> The measured value of the cell parameter,  $c \sim 15.3 \text{ \AA}$ , is compatible with a four (AO) layer misfit compound. This specific lattice thus comes from the coexistence of two subcells  $S_1$  and  $S_2$ , associated with  $[\text{Bi}_2\text{Ba}_2\text{O}_4]^{\text{RS}}$  layers and one  $[\text{RhO}_2]^{\text{CdI}_2}$  layer, respectively [Fig. 1(c)]. The Rh based compound exhibits a misfit ratio  $b_1/b_2$  close to 1.8, in contrast to the isotype  $\text{BiBaCoO}$  misfit cobaltite, which is commensurate with  $b_1/b_2 = 2$ .<sup>14</sup> Consequently, taking into account the average “ $\text{Bi}_{2.02}\text{Ba}_2\text{Rh}_{1.98}$ ” composition, deduced from the EDS analysis coupled to electron diffraction, in good agreement with the nominal one, the final formula  $[\text{Bi}_{1.95}\text{Ba}_{1.95}\text{Rh}_{0.1}\text{O}_4][\text{RhO}_2]_{1.8}$  is deduced. It must be emphasized that, according to the larger ionic radius of  $\text{Rh}^{4+}/\text{Rh}^{3+}$  than the low spin  $\text{Co}^{4+}/\text{Co}^{3+}$ , the expansion of the  $\text{CdI}_2$  type subcell creates a decrease of the  $b_1/b_2$  ratio with  $b_1/b_2 = 1.8$  compared to 2 for the Co misfit.

### Resistivity: $T$ and $H$ dependencies

The resistivity of the  $[\text{Bi}_{1.95}\text{Ba}_{1.95}\text{Rh}_{0.1}\text{O}_4][\text{RhO}_2]_{1.8}$  misfit ceramic, made of randomly distributed microcrystals, is plotted in Fig. 2. The curve shows a metalliclike behavior of the resistivity from 400 K down to 40 K with a value of 17 m $\Omega$  cm at room temperature. At 40 K the value of the resistivity is minimal, close to 5.5 m $\Omega$  cm. Below this temperature, the resistivity increases with a value of 13 m $\Omega$  cm at 5 K. The results of Fig. 2 fit well with the recently published results.<sup>13</sup> Due to the large electrical anisotropy of misfit cobalt oxides with metallic in-plane and insulating out-of-plane resistivities ( $\rho_c/\rho_{ab} \sim 10^2\text{--}10^4$ ), the transport measurements of ceramic misfit cobalt oxide samples are representative of the in-plane component.<sup>15,16</sup> The same results should apply in the case of Rh samples, due to the similarity

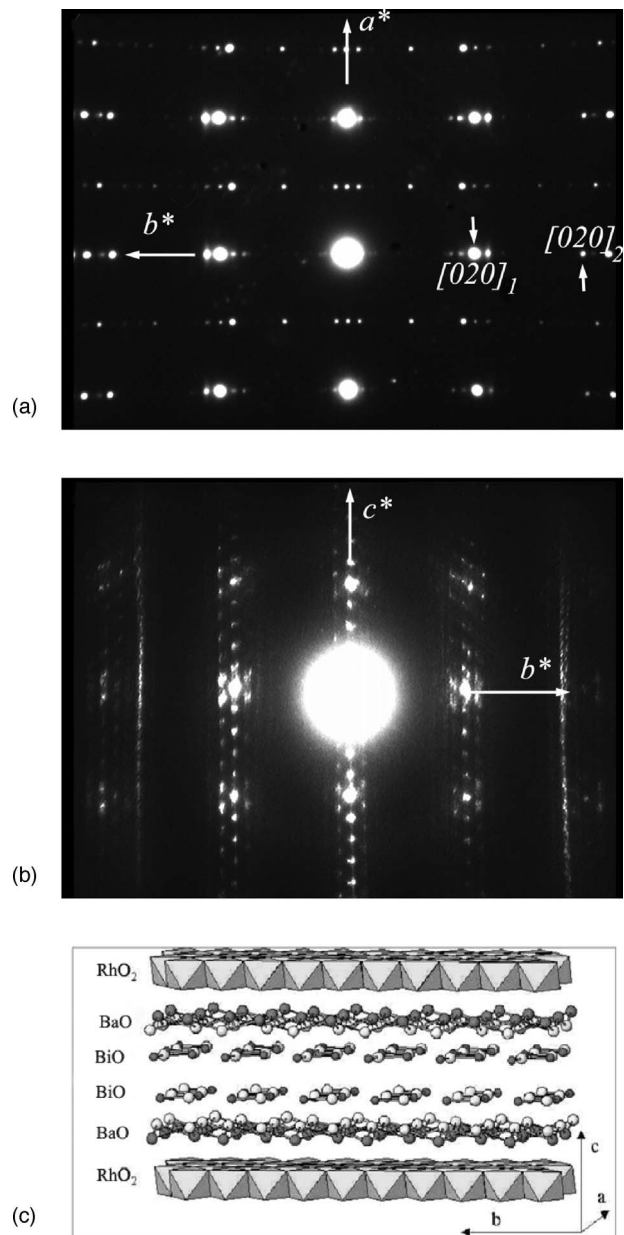


FIG. 1. Experimental [001] (a) and [100] (b) ED patterns. The two subcells, rocksalt and  $\text{CdI}_2$ -like, labelled 1 and 2, respectively, are shown with white arrows. The second set of extra spots characteristic of double  $(\text{BiO})_\infty$  layers based modulated structure is clearly visible in the [100] pattern. (c) Schematic picture of the rhodate misfit layer structure showing the intergrowth of the two sublattices.

in crystallographic structure. However, crystal growth will be necessary to confirm this hypothesis.

The inset of Fig. 2 shows the magnetoresistance  $\text{MR}(\%) = 100 \times [\rho(H) - \rho(0 \text{ T})] / \rho(0 \text{ T})$  vs temperature curve for different applied fields of 3.5 T, 7 T, and 14 T. Upon application of an external magnetic field of 7 T, the MR is almost 0% even at low temperature. For 3.5 T and 14 T, the resistivity is decreased (–1% at 5 K) or increased (+5% at 5 K), respectively, by the application of the field.

To clarify this behavior, the resistivity has been measured at constant  $T$  ( $T \leq 15 \text{ K}$ ) in the magnetic field varying from

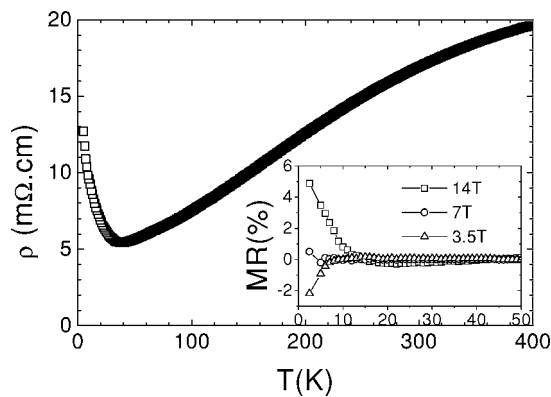


FIG. 2. Resistivity vs temperature curve of  $[\text{Bi}_{1.95}\text{Ba}_{1.95}\text{Rh}_{0.1}\text{O}_4][\text{RhO}_2]_{1.8}$ . Inset: corresponding  $T$  dependence of the magnetoresistance (MR) for three different magnetic fields (3.5 T, 7 T, and 14 T); for the sake of clarity only the low  $T$  part is shown.

0 to 14 T (Fig. 3). Up to  $\mu_0 H \sim 3$  T, resistivity decreases as the field increases. Such a negative magnetoresistance has often been observed in cobalt misfit oxides.<sup>10,15,16</sup> After reaching a minimum (depending on the temperature) the MR starts to increase and becomes positive. For  $T=5$  K, the MR goes through zero for a field close to 6.5 T. We can notice that the positive MR in 14 T does not exceed +5% in magnitude even at 2.5 K. This is completely different from  $\text{Ca}_3\text{Co}_4\text{O}_9$  and  $\text{BiCaCoO}$  for which the magnetoresistance reaches -35% (Ref. 15) and -60% (Ref. 16), respectively, in 7 T. Nonetheless a positive MR was reported for  $[\text{Bi}_2\text{Ba}_{1.8}\text{Co}_{0.2}\text{O}_4][\text{CoO}_2]_2$  reaching +10% in 7 T.<sup>14</sup>

#### Thermopower: $T$ and $H$ dependencies

The thermoelectric power of the  $[\text{Bi}_{1.95}\text{Ba}_{1.95}\text{Rh}_{0.1}\text{O}_4][\text{RhO}_2]_{1.8}$  misfit rhodate is plotted in Fig. 4 as a function of  $T$ . The Seebeck coefficient is a powerful technique to investigate the electronic properties of ceramics, as it is not sensitive to grain boundaries.  $S$  is increasing continuously from 0 to 150 K and then reaches an almost constant value of +95  $\mu\text{V}/\text{K}$  up to 300 K. On the same curve, the  $S$  values of  $\text{BiBaCoO}$  are also reported.<sup>14</sup> It is found that in the region  $T > 40$  K, the thermopower of the two samples are very close. In the case of cobalt oxides, the similar Seebeck coef-

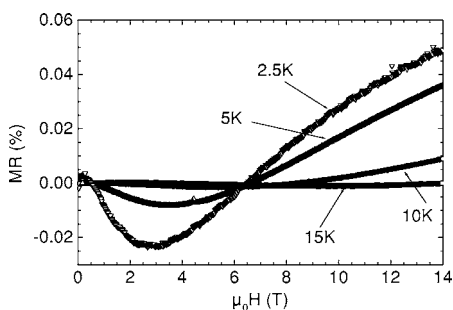


FIG. 3. Magnetic field ( $H$ ) dependence of the MR for four temperatures (2.5 K, 5 K, 10 K, and 15 K). The resistivity measurements have been made in a zero field cooling mode.

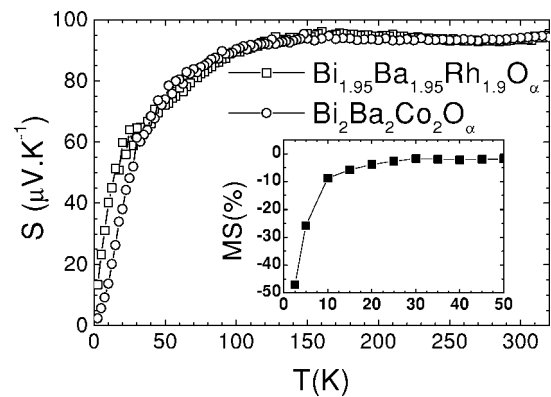


FIG. 4. Thermoelectric power of  $[\text{Bi}_{1.95}\text{Ba}_{1.95}\text{Rh}_{0.1}\text{O}_4][\text{RhO}_2]_{1.8}$  and  $[\text{Bi}_2\text{Ba}_{1.8}\text{Co}_{0.2}\text{O}_4][\text{CoO}_2]_2$  (from Ref. 14). Inset: corresponding  $T$  dependence of the magnetothermopower (MS) of  $\text{BiBaRhO}$  for a 9 T magnetic field; for the sake of clarity only the low  $T$  part is shown.

ficients measured in  $\text{Na}_x\text{CoO}_2$  and misfit cobaltites reflects the properties of the conducting  $\text{CoO}_2$  layers.<sup>1,3-6</sup> In the case of rhodium misfits, according to the layer structure and as previously discussed for the resistivity, the thermoelectric power should also be dominated by the  $\text{RhO}_2$  layers. This property can be understood from the formula established by Bergman *et al.* for a material made of a mixture of two phases, one metallic and one insulating,<sup>17</sup>

$$S_E = S_M + (S_I - S_M) \left[ \frac{\left( \frac{\kappa_E/\kappa_M}{\sigma_E/\sigma_M} - 1 \right)}{\left( \frac{\kappa_I/\kappa_M}{\sigma_I/\sigma_M} - 1 \right)} \right],$$

where  $S_E$ ,  $\sigma_E$ ,  $\kappa_E$  ( $S_M$ ,  $\sigma_M$ ,  $\kappa_M$ ;  $S_I$ ,  $\sigma_I$ ,  $\kappa_I$ ) are the Seebeck coefficient, electrical conductivity, and thermal conductivity of the composite material, the metallic and the insulating parts, respectively. In the case of misfits,  $\sigma_I/\sigma_M = \sigma_c/\sigma_{ab} \sim 10^{-2} - 10^{-4}$ , and  $\kappa_I/\kappa_M \sim 10^{-1}$ ,<sup>18</sup> so that the Seebeck coefficient is  $S_E \sim S_M = S_{ab}$ .

The  $S$  values are very close in Fig. 4 for cobalt and rhodium misfits above 40 K which confirm the similar role played by the  $\text{CoO}_2$  and  $\text{RhO}_2$  layers. However, for the lowest temperatures, the  $S$  value of  $\text{BiBaRhO}$  remains high ( $S \sim 23 \mu\text{V K}^{-1}$  at 5 K) as compared to  $\text{BiBaCoO}$  ( $S \sim 6 \mu\text{V K}^{-1}$  at 5 K).

Large Seebeck values as  $T \rightarrow 0$  have already been reported in the case of  $\text{BiCaCoO}$  and in  $\text{BiPbCaCoO}$  (Ref. 10) and they are strongly magnetic field dependent. For  $\text{BiBaRhO}$ , the dependence of  $S$  versus field has thus been investigated. The inset of Fig. 4 shows the magnetothermopower for low temperatures in a 9 T field,  $\text{MS}(\%) = 100^* [S(9 \text{ T}) - S(0 \text{ T})] / S(0 \text{ T})$ . MS starts to decrease at 30 K with a strong temperature dependence and rises to -45% at 2.5 K. This effect has been confirmed by the thermoelectric power measurements in fields varying from -9 T to 9 T at 2.5 K and 5 K (Fig. 5). At 2.5 K, the thermopower decreases almost linearly upon magnetic field application from 17  $\mu\text{V K}^{-1}$  in 0 T down to 9  $\mu\text{V K}^{-1}$  in 9 T resulting in a 47% variation. This is completely different from the  $\rho(H)$  curves (Fig. 3), where the MR is first decreasing, then increasing with field. While the MR values are quite small, the

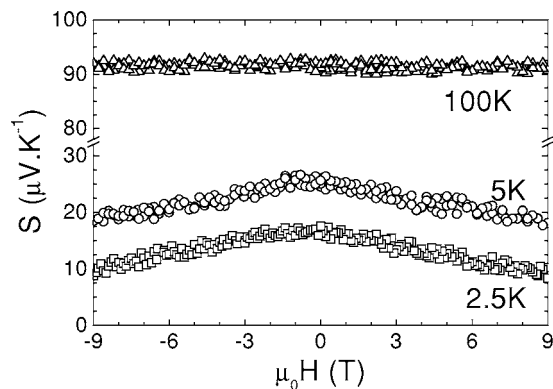


FIG. 5. Magnetic field ( $H$ ) dependence of the MS for two temperatures (2.5 K and 5 K). The thermopower measurements have been made in a zero field cooling mode.

field can induce a significant effect on the thermoelectric power.

### Specific heat

The electronic contribution to the specific heat has been extracted by plotting  $C/T$  against  $T^2$  in the low  $T$  regime for which the lattice contribution can be well approximated by a cubic term (Fig. 6). Apart from a small upturn for  $T < 3$  K which may originate from an hyperfine contribution, the curve of Fig. 6 can be fitted by using the expression  $C/T = \gamma + \beta T^2$ , where  $\gamma$  and  $\beta$  originate from charge carriers and from phonons, respectively. We find  $\gamma = 38 \text{ mJ K}^{-2} \text{ mol}(\text{Rh})^{-1}$  and  $\beta = 3.16 \text{ mJ K}^{-4} \text{ mol}^{-1}$ . In comparison to BiBaCoO, for which  $\gamma = 22 \text{ mJ K}^{-2} \text{ mol}(\text{Co})^{-1}$  (Ref. 14) and  $\text{Ca}_3\text{Co}_4\text{O}_9$  with  $\gamma = 37 \text{ mJ K}^{-2} \text{ mol}(\text{Co})^{-1}$ ,<sup>9</sup> the value obtained for BiBaRhO indicates that the electron correlations are not strongly affected by the Rh for Co substitution.

### Susceptibility

The inverse magnetic susceptibility  $\chi^{-1}$  of the Ba-based rhodate is plotted in Fig. 7. BiBaRhO shows a quasiparamag-

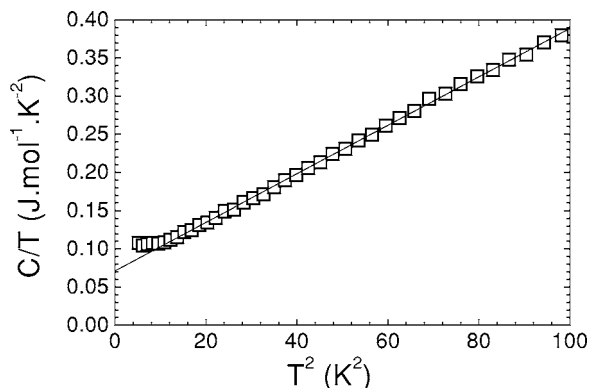


FIG. 6.  $T^2$  dependence of the molar  $C/T$  ratio for the  $[\text{Bi}_{1.95}\text{Ba}_{1.95}\text{Rh}_{0.1}\text{O}_4][\text{RhO}_2]_{1.8}$  rhodate. The electronic and phononic specific-heat coefficients have been deduced according to the fitting curve (solid curve).

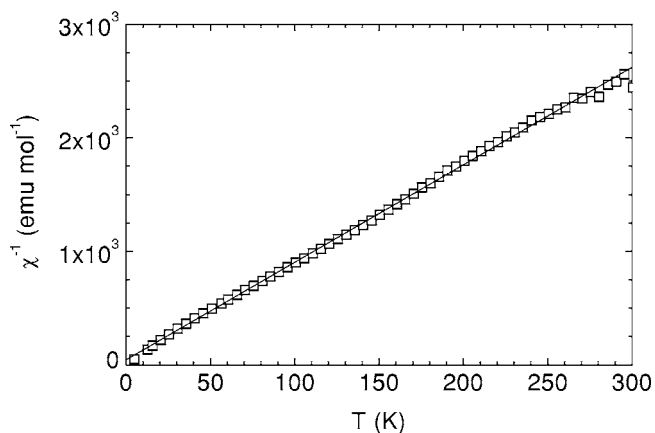


FIG. 7. Temperature dependence of the molar magnetic inverse susceptibility  $\chi^{-1}$ , for the  $[\text{Bi}_{1.95}\text{Ba}_{1.95}\text{Rh}_{0.1}\text{O}_4][\text{RhO}_2]_{1.8}$  ceramic sample ( $\mu_0 H = 0.3$  T). The solid line is a fit of the experimental data following  $\chi = C/(T + \theta_p)$ . The data have been corrected from the sample holder contribution.

netic behavior and no transition is observed, in contrast to BiBaCoO.<sup>14</sup> From the Curie-Weiss law, the effective moment per rhodium element is evaluated at  $\mu_{\text{eff}} \sim 0.7 \mu_B/\text{Rh}$  with a small antiferromagnetic  $\theta_p \approx -5.3$  K.

### COMPARISON WITH THE Co MISFITS AND DISCUSSION

The resistivities ( $\rho$ ) of the BiBaRhO and BiBaCoO systems show a similar reentrance at low  $T$  with a minimum at 40 K (Rh) and 100 K (Co), a metallic response above this minimum and a small increase of  $\rho$  below ( $\rho_{300 \text{ K}}/\rho_{\text{min}} \sim 5$ ). The values of  $\rho$  are in the same range of 15–30 m $\Omega$  cm at room temperature. The similar conducting behaviors suggest that Rh plays exactly the same role as the isoelectronic cobalt cation in the  $\text{CoO}_2$  layers.

For  $T > 40$  K, the thermopower curves of BiBaRhO and BiBaCoO are completely superimposed and above 100 K, a constant value of  $+95 \mu\text{V}/\text{K}$  is obtained in both compounds up to room temperature. From the generalized Heikes formula, the Seebeck coefficient can be calculated at  $T \rightarrow \infty$ , but the formula is valid only in the case of localized carriers. Nevertheless, if we suppose that  $S$  remains constant up to higher temperature (this is usually the case in Co misfits), it can be used to crudely estimate the room temperature value of  $S$ ,<sup>7</sup> with

$$S = -\frac{k_B}{e} \ln\left(\frac{g_3}{g_4} \frac{1-x}{x}\right)$$

where  $x$  is the  $\text{Co}^{3+}$  (here  $\text{Rh}^{4+}$ ) concentration of the  $\text{CoO}_2$  ( $\text{RhO}_2$ ) layer, and  $g_3$  and  $g_4$  are the low spin degeneracies of  $\text{Co}^{3+}/\text{Co}^{4+}$  ( $\text{Rh}^{3+}/\text{Rh}^{4+}$ ). The same  $S$  value is consistent with the same electronic configurations of  $\text{Rh}^{3+}/\text{Rh}^{4+}$  and  $\text{Co}^{3+}/\text{Co}^{4+}$ , inducing the same spin degeneracies ( $g_3 = 1$  and  $g_4 = 6$ ), and with  $x \sim 0.33$  for the two compounds. If we have a low-spin  $\text{Rh}^{3+}$  ( $S = 0$ ) in the NaCl-like layers, the 67%  $\text{Rh}^{4+}$  ( $S = 1/2$ ) of the  $\text{CdI}_2$  layers would be responsible for an effective magnetic moment  $\mu_{\text{eff}} \sim 1.42 \mu_B/\text{Rh}$  of the misfit for-



mula. This value is different from the  $0.70 \mu_B/\text{Rh}$  evaluated from the Curie-Weiss analysis of the susceptibility curve. This underlines the limit of applicability of the Heikes formula for such complex redox systems. It was previously shown that the Seebeck coefficient strongly depends on the  $b_1/b_2$  parameter because this ratio is directly linked to the doping level in these materials.<sup>19</sup> We find here exactly the same Seebeck coefficient at high  $T$  even if the  $b_1/b_2$  ratios are different. This suggests that the oxygen stoichiometry of BiBaRhO and BiBaCoO might be different so that the cobalt and rhodium valency ( $x$ ) in the CdI<sub>2</sub> layers can be the same. Oxygen nonstoichiometry has already been analyzed in Ca<sub>3</sub>Co<sub>4</sub>O<sub>9</sub> (Ref. 20) and a comparison of BiBaRhO and BiBaCoO would be very instructive.

From the resistivity curves and the Seebeck coefficients above 40 K, we can thus conclude that Rh<sup>3+</sup>/Rh<sup>4+</sup> plays exactly the same role as Co<sup>3+</sup>/Co<sup>4+</sup>, reinforcing the importance of electronic configuration and spin degeneracy on the transport properties. However, at low  $T$ , below 40 K, differences are observed. In contrast to the high temperature behavior, the Seebeck coefficient below 40 K is larger in the case of BiBaRhO than in BiBaCoO. As shown in the inset of Figs. 4 and 5, the large  $S$  value can be decreased by a magnetic field. Such a large magnetothermopower as large as  $-50\%$  has already been reported in BiCaCoO.<sup>10</sup> In this material, this large MS was coexisting with a large negative MR. Here, on the contrary, the MR is small, and MR and MS are not so clearly related.

The magnetoresistance measured in the polycrystalline BiBaRhO misfit rhodate is completely different from the previous measurements reported in misfit cobaltites. By comparison the MR of the homologous BiBaCoO ceramic is positive even at low fields and shows a linear dependence on  $H$  at high fields.<sup>14</sup> In polycrystals, the MR can be small and positive up to 9 T [BiBaCoO (Ref. 14) and TlSrCoO (Ref. 21)], or large and negative [see, for example, BiCaCoO (Ref. 10)]. The origin of the two components observed in Fig. 3 is unclear. It has been recently shown that in another cobalt misfit, the Pb-doped BiSrCoO single crystals, two components coexist<sup>22</sup> for both the in-plane and out-of-plane MR. The negative one would come from the reduction of the spin scattering of charge carriers, while the positive one might be related to the complex magnetic structure arising from antiferromagnetic short-range fluctuations.<sup>22</sup> In the related compound Na <sub>$x$</sub> CoO<sub>2</sub>, two components have also been measured, which strongly depend on the current and field orientations.<sup>23</sup>

In the BiBaRhO polycrystals, the two components proposed by Luo *et al.* might be effective, as antiferromagnetic fluctuations are present. Nevertheless, we have to be careful with interpretations and models because our measurements are made on nonoriented ceramics containing grain boundaries and so, they produce average results.

The most important point is that MR is observed in these rhodium oxides. Very few reports exist on the transport properties of rhodium oxides (some examples are given in Ref. 24) and to our knowledge, only one publication<sup>25</sup> showed the resistivity of a rhodium oxide SrRhO<sub>3</sub> upon external magnetic field application. A clear lack of magnetoresistance was observed. In this case of SrRhO<sub>3</sub> perovskite, the magnetoresistance is equal to zero. Thus, the MR observed in the present misfit rhodate is unique. It shows that the CdI<sub>2</sub> layer plays a peculiar role in the transport properties and can promote the appearance of MR in these materials.

The magnetic properties of the CdI<sub>2</sub> like layers remain unclear. The specific heat and the susceptibility curves reveal that no long range ordering exists in these materials. The formation of spin density waves below 100 K has been proposed in the cobalt misfits<sup>26</sup> but pseudogap formation<sup>27</sup> has also been claimed. The rhodium misfits are a new example of the puzzling magnetism induced by the spins  $S=1/2$  on these triangular lattices, where frustration is a crucial parameter.

## CONCLUSION

The magnetotransport properties of [Bi<sub>1.95</sub>Ba<sub>1.95</sub>Rh<sub>0.1</sub>O<sub>4</sub>] [RhO<sub>2</sub>]<sub>1.8</sub> have been investigated. The high temperature transport properties are very similar to the ones of the isostructural [Bi<sub>2</sub>Ba<sub>1.8</sub>Co<sub>0.2</sub>O<sub>4</sub>][CoO<sub>2</sub>]<sub>2</sub>. The material is metallic above 40 K, with a large Seebeck coefficient of  $+95 \mu\text{V}/\text{K}$  at room temperature. Rh<sup>3+/4+</sup> and Co<sup>3+/4+</sup> which are isoelectronic ( $t_{2g}^6$  and  $t_{2g}^5$ ) thus have the same role for the high temperature transport, confirming that Co<sup>3+/4+</sup> is low spin in the case of cobalt misfit oxides. The specific heat coefficient  $\gamma = 38 \text{ mJ K}^{-2} \text{ mol}^{-1}$  moderately reflects strong electronic correlations as in BiBaCoO.

In contrast, below 40 K, the two compounds are different. The Seebeck coefficient of the rhodium misfit is increased by a term which is strongly magnetic field dependent. Also, the MR, which was positive for BiBaCoO, is now replaced by a small positive MR in the high field and a negative one at low field. This is, to our knowledge, the first example of MR in rhodium oxides, emphasizing the richness of the transport properties associated with the CdI<sub>2</sub>-type layers.

<sup>1</sup>I. Terasaki, Y. Sasago, and K. Uchinokura, Phys. Rev. B **56**, R12685 (1997).

<sup>2</sup>K. Takada, H. Sakurai, E. Takayama-Muromachi, F. Izumi, R. A. Dilanian, and T. Sasaki, Nature (London) **422**, 53 (2003).

<sup>3</sup>A. Maignan, S. Hébert, D. Pelloquin, C. Michel, and J. Hejtmanek, J. Appl. Phys. **92**, 1964 (2002).

<sup>4</sup>R. Funahashi and M. Shikano, Appl. Phys. Lett. **81**, 1459 (2002).

<sup>5</sup>S. Horii, I. Matsubara, M. Sano, K. Fujie, M. Suzuki, R.

Funahashi, M. Shikano, W. Shin, N. Murayama, J. Shimoyama, and K. Kishio, Jpn. J. Appl. Phys., Part 1 **42**, 7018 (2003).

<sup>6</sup>I. Matsubara, R. Funahashi, T. Takeuchi, S. Sodeoka, T. Shimizu, and K. Ueno, Appl. Phys. Lett. **78**, 3627 (2001).

<sup>7</sup>W. Koshibae, K. Tsutsui, and S. Maekawa, Phys. Rev. B **62**, 6869 (2000).

<sup>8</sup>D. J. Singh, Phys. Rev. B **61**, 13397 (2000).

<sup>9</sup>P. Limelette, V. Hardy, P. Auban-Senzier, D. Jérôme, D. Flahaut,

- S. Hébert, R. Frésard, Ch. Simon, J. Noudem, and A. Maignan, *Phys. Rev. B* **71**, 233108 (2005).
- <sup>10</sup>A. Maignan, S. Hébert, M. Hervieu, C. Michel, D. Pelloquin, and D. Khomskii, *J. Phys.: Condens. Matter* **15**, 2711 (2003).
- <sup>11</sup>P. Limelette, S. Hébert, V. Hardy, R. Frésard, Ch. Simon, and A. Maignan (unpublished).
- <sup>12</sup>D. Pelloquin, S. Hébert, A. Maignan, and B. Raveau, *J. Solid State Chem.* **178**, 769 (2005).
- <sup>13</sup>S. Okada and I. Terasaki, *Jpn. J. Appl. Phys., Part 1* **44**, 1834 (2005).
- <sup>14</sup>M. Hervieu, A. Maignan, C. Michel, V. Hardy, N. Créon, and B. Raveau, *Phys. Rev. B* **67**, 045112 (2003).
- <sup>15</sup>A. C. Masset, C. Michel, A. Maignan, M. Hervieu, O. Toulemonde, F. Studer, B. Raveau, and J. Hejtmanek, *Phys. Rev. B* **62**, 166 (2000).
- <sup>16</sup>T. Yamamoto, K. Uchinokura, and I. Tsukada, *Phys. Rev. B* **65**, 184434 (2002).
- <sup>17</sup>D. J. Bergman and O. Levy, *J. Appl. Phys.* **70**, 6821 (1991).
- <sup>18</sup>I. Terasaki, H. Tanaka, A. Satake, S. Okada, and T. Fujii, *Phys. Rev. B* **70**, 214106 (2004).
- <sup>19</sup>A. Maignan, D. Pelloquin, S. Hébert, Y. Klein, and M. Hervieu, in *Proceedings of the 23rd International Conference on Thermoelectrics* (2004).
- <sup>20</sup>M. Karpinnen, H. Fjellvag, T. Konno, Y. Morita, T. Motohashi, and H. Yamauchi, *Chem. Mater.* **16**, 2790 (2004).
- <sup>21</sup>S. Hébert, S. Lambert, D. Pelloquin, and A. Maignan, *Phys. Rev. B* **64**, 172101 (2001).
- <sup>22</sup>X. G. Luo, X. H. Chen, G. Y. Wang, C. H. Wang, X. Li, W. J. Miao, G. Wu, and Y. M. Xiong, *cond-mat/0412623* (2004).
- <sup>23</sup>C. H. Wang, X. H. Chen, J. L. Luo, G. T. Liu, X. X. Lu, H. T. Zhang, G. Y. Wang, X. G. Luo, and N. L. Wang, *Phys. Rev. B* **71**, 224515 (2005).
- <sup>24</sup>T. Nakamura, T. Shimura, M. Itoh, and Y. Takeda, *J. Solid State Chem.* **103**, 523 (1993); T. Shimura, M. Itoh, Y. Inaguma, and T. Nakamura, *Phys. Rev. B* **49**, 5591 (1994); R. Horyn, Z. Bukowski, M. Wolcyrz, and A. J. Zaleski, *J. Alloys Compd.* **262-263**, 267 (1997).
- <sup>25</sup>K. Yamaura and E. Takayama-Muromachi, *Phys. Rev. B* **64**, 224424 (2001).
- <sup>26</sup>J. Sugiyama, J. H. Brewer, E. J. Ansaldo, H. Itahara, K. Dohmae, Y. Seno, C. Xia, and T. Tani, *Phys. Rev. B* **68**, 134423 (2003).
- <sup>27</sup>I. Terasaki, *Mater. Trans., JIM* **42**, 951 (2001).